Thermoelectric power of bismuth nanowires

J. Heremans and C. M. Thrush
General Motors Research and Development Center, Physics and Physical Chemistry Department, Warren, Michigan 48090-9055
(Received 30 November 1998; revised manuscript received 26 January 1999)

We report here measurements of the thermoelectric power and longitudinal magneto-Seebeck coefficient of 200 nm diameter single-crystal bismuth nanowires. Nanowires of pure Bi and of *n*-type-doped Bi (with Te at about $5\times10^{18}\,\mathrm{cm}^{-3}$) were measured. The wires are imbedded in porous anodic alumina. The data are taken on arrays of wires connected in parallel, at temperatures from 8 to 300 K, and, between 10 and 80 K, in magnetic fields from 0 to 5 Tesla. It has been theoretically calculated that bismuth nanowires should have a strongly increased thermoelectric figure of merit over bulk Bi, when the diameter is decreased below about 10 nm. The nanowires in this study were selected because they are easier to prepare and handle. The temperature-dependent thermopower data are consistent with the partial electron and hole thermopower values calculated using the carrier Fermi energies obtained from Shubnikov–de Haas oscillations on the same samples. [S0163-1829(99)01919-0]

INTRODUCTION

Theoretical calculations[1] predict that nanowires of the semimetal bismuth should have an enhanced thermoelectric figure of merit. According to those calculations, an array of nanowires oriented along the trigonal direction with diameters on the order of 7 nm could have figure of merit ($Z.T\approx2$ at 300 K), which would be large enough to make a thermoelectric cooler with an efficiency approaching that of a vapor-compression unit. The thermoelectric power, thermal conductivity and electrical conductivity of bulk single-crystal Bi were reported, in the 80 to 300 K range, by Gallo, Chandrasekhar, and Sutter,[2] and extended to low and ultralow temperatures in Refs. 3–7. A review of these properties is given in Ref. 8. The magneto-Seebeck coefficients have been measured in longitudinal[9] and transverse[10] magnetic fields. The low-field thermomagnetic coefficients[11] have been used to determine[12] the temperature dependence of the nonparabolic band structure up to 300 K. More recently, attention has focused on the galvanomagnetic properties of single-crystal nanowire arrays of Bi, with wire diameters first in the submicron range[13] and then in the 28–110 nm (Refs. 14 and 15) range. In particular, a semimetal-to-semiconductor transition was observed[14] as the wire diameter is decreased from 100 to 60 nm, and electron localization effects become visible[15] in wires of diameters below 50 nm. The purpose of this paper is to present the first experimental data on thermoelectric power and longitudinal thermomagnetic coefficients of an array of single-crystal Bi nanowires with a diameter of 200 nm. The nanowire array is imbedded in porous amorphous alumina.

EXPERIMENT

The samples consist of a porous amorphous alumina host material prepared by anodic oxidation of aluminum, commercially available as Whatman Anodisc. This is an alumina plate, about 50-μm thick, which contains hexagonal-like arrays of holes, 200 ± 25 nm in diameter, about 400 nm apart. The holes are straight and connect one face of the sample to the other. Six-nine pure Bi is introduced into this host material by a vapor-phase technique[16] described elsewhere. A sample of Bi *n*-type doped with Te was also prepared from a melt that contained approximately $3\times10^{17}\,\mathrm{cm}^{-3}$ atoms of Te, though the density of the Te donors incorporated into the nanowires will be shown to be an order of magnitude larger. A cross-sectional scanning electron micrograph of a representative sample is shown in Ref. 15. The Bi wires are single crystals, with their long axis oriented in the [0, 0.949, 0.315] direction in the rhombohedral [*x*,*y*,*z*] system, where the directions are $x=$binary, $y=$bisectrix, and $z=$trigonal, as in previous[14,15,16] work. The sample orientation is about 18.4° from the bisectrix axis, $\varphi=71.6°$ from the trigonal axis. Along this direction, the electrical conductivity σ, thermal conductivity κ and thermoelectric power α can be expressed as function of the same quantities along the bisectrix (index 2) and trigonal (index 3) directions and angle φ between the wire axis and the trigonal direction as[2]

$$\sigma(\varphi)=\sigma_2+(\sigma_3-\sigma_2)\cos^2(\varphi), \tag{1}$$

$$\kappa(\varphi)=\kappa_2+(\kappa_3-\kappa_2)\cos^2(\varphi), \tag{2}$$

$$\alpha(\varphi)=\alpha_2+\frac{\kappa_2}{\kappa_3}\frac{(\alpha_3-\alpha_2)\cos^2(\varphi)}{1+(\kappa_2/\kappa_3-1)\cos^2(\varphi)}. \tag{3}$$

Since the host material is amorphous, the Bi wires conduct most of the heat. The lattice thermal conductivity dominates the electronic contribution in bulk Bi, and $\kappa_2/\kappa_3\approx1.67$ at $T>50\,\mathrm{K}$.[2] In nanowires, if the scattering of phonons on the wire walls is partially diffuse, the phonon mean-free path is partially limited by the wire diameter, and the κ_2/κ_3 ratio will be bounded by the ratio of the sound velocities v of the dominant acoustic phonon mode. The average of v_2/v_3 over longitudinal and transverse modes is about 1.3 using the sound velocity values of Eckstein, Lawson, and Renecker,[17] and $1.3\leqslant\kappa_2/\kappa_3\leqslant1.7$. Using $\kappa_2/\kappa_3=1.67$, bisectrix value of the transport coefficient dominates the value along the wire direction by a ratio of 90% to 10% for the conductivities and

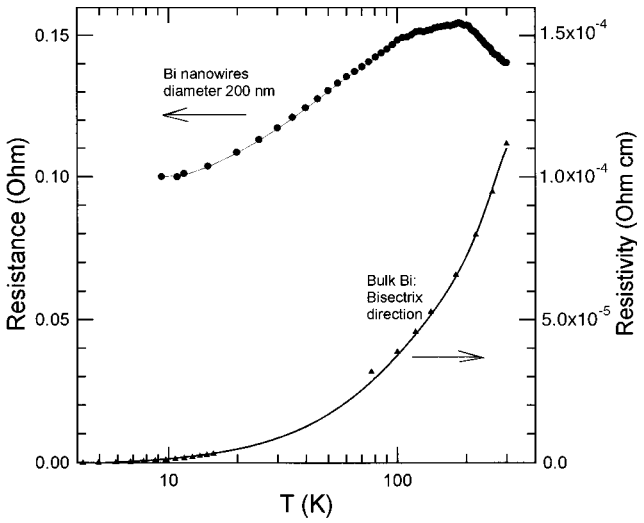

FIG. 1. The resistance of an array of 200 nm diameter pure Bi nanowires as a function of temperature (left ordinate) and the resistivity of bulk Bi (right ordinate) along the bisectrix direction (Ref. 3).

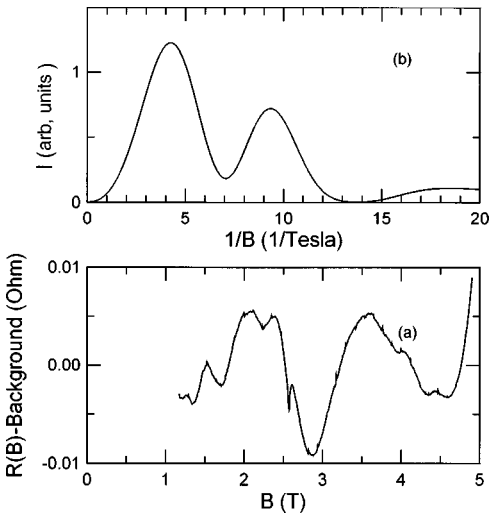

FIG. 2. (a) Magnetic-field dependence of the oscillating part of the magnetoresistance of the array of Ag paint-mounted pure Bi nanowires used for thermopower measurements, after the background magnetoresistance, similar to that in Ref. 14, was subtracted using a third order polynomial fit. (b) Fourier transform of the oscillatory part of the magnetoresistance. The magnetic field is parallel to the wire axis.

88% to 12% for the thermopower. Therefore, it is convenient to compare the following data on nanowires to those on bulk Bi along the bisectrix axis.

The data reported were measured on two samples prepared from pure Bi, one mounted with Ag-filled epoxy (sample 1) and one mounted with Wood's metal (sample 2). Sample 3 was prepared from Te-doped Bi, and mounted like sample 1. The experiments are two-probe measurements, which raises concerns about the contact resistances. The use of two different mounting procedures gives an indication of the influence of the contact resistance, which will be discussed separately for each transport property. The bottom face of the Bi-impregnated alumina plate was mounted on a hexagonal pyrolytic BN substrate with either Wood's metal or Ag epoxy. A roughly $2.5\times2.5\,\mathrm{mm}^2$ gold plate was soldered to its top surface with Wood's metal. A thin-foil chromel/constantan thermocouple was mounted differentially between the top Au plate and the BN substrate. Two thin Au wires were soldered to the Au plate, one for current and one for voltage leads, and similarly two Au wires made contact to the bottom side of the alumina plate. The thermoelectric power of the Au wires is on the order of $+1\ \mu$V/K, and, because this quantity is much smaller than the thermopower values for Bi and contains a large phonon-drag contribution, which may be sample dependent, it will be ignored in the data reported later. A very small 120 Ω strain gage was varnished onto the Au plate as a heater. The BN substrate with this construction was attached to a liquid He cryostat and data are taken in a magnetic field of 0 to 5 T at temperatures below 75 K, and in zero field up to room temperature. It is a limitation of the cryostat design that the superconducting magnet cannot be energized to full field when the sample insert is above 75 K.

RESULTS AND DISCUSSION

Figure 1 shows the electrical resistance of an array 200 nm pure Bi nanowires mounted with Wood's metal. The data on sample 1 are similar, though the room temperature value is 0.23 Ω and the data are noisier. As in previous work[14,15] on arrays of wires, it is impossible to estimate the number of wires connected in parallel between the top Au plate and the BN substrate, and thus, the resistance of an individual nanowire cannot be determined. We note the similarity of the temperature dependence curve to that in Ref. 13, and conclude that the contact resistance between the Wood's metal or the Ag paint and the Bi wires does not dominate the relative resistance data reported. The magnetoresistance curves are similar to those reported previously[14] on semimetallic wires, but for this study we used a much smaller scanning step in magnetic field, in order to evidence the quantum oscillations at 4.2 K. At fields at which the cyclotron radius is smaller than the wire diameter, these are Shubnikov–de Haas (SdH) oscillations,[13] shown in Fig. 2(a) for sample 1. A Fourier transform of this oscillating part of the magnetoresistance is shown in Fig. 2(b), and shows two periods, at 4.2 and at 9.3 T^{-1}. The SdH frequency is given, as a function of the cyclotron mass m_c at the band edge by

$$\frac{1}{\Delta\left(\frac{1}{B}\right)}=\frac{m_c\cdot\gamma(E_F)}{\hbar q}, \tag{4}$$

where the function $\gamma(E_F)$ includes the effect of band nonparabolicity,[12] which is important for electrons at the L point of the Brillouin zone. For electrons, $\gamma(E_F^e)$ is defined by

$$\gamma(E_F^e)=E_F^e\left(1+\frac{E_F^e}{E_g}\right) \tag{5}$$

while its derivative with respect to energy is

$$\gamma'(E_F^e)=\left(1+2\frac{E_F^e}{E_g}\right), \tag{6}$$

TABLE I. Experimental SdH periods, associated carrier Fermi energies and densities, and calculated partial and total thermopower slopes for the three Bi nanowire samples (Sample 1 is pure Bi, mounted with Ag paint, sample 2 is pure Bi mounted with Wood's metal, and sample 3 is Bi:Te at about $5\times10^{18}\,\mathrm{cm}^{-3}$). Also shown are literature values for the same quantities in bulk Bi, and the corresponding thermopower along the [0, 0.949, 0.315] axis.

Property	Units	Bulk Bi	Sample 1	Sample 2	Sample 3
SdH period	(Tesla^{-1})		9.25		na
E_F^h (Holes)	(meV)	10.8[12]	7.8		na
P	(cm^{-3})	2.7×10^{17}	1.7×10^{17}		na
SdH period	(Tesla^{-1})				14.6
E_F^{Le} (Light electrons)	(meV)	27.2[12]			97
SdH period	(Tesla^{-1})		4.2	4.0	19.5
E_F^{He} (Heavy electrons)	(meV)	27.2[12]	36	35	84
N	(cm^{-3})	2.7×10^{17}	5.5×10^{17}	5.0×10^{17}	5×10^{18}
α_e/T	($\mu\mathrm{V/K}^2$)	-1.62[12]	-1.2		-0.51 ± 0.04
α_h/T	($\mu\mathrm{V/K}^2$)	2.231[12]	3.2		na
Calculated α/T	($\mu\mathrm{V/K}^2$)	-0.66	-0.09		-0.51 ± 0.04
Experimental α/T	($\mu\mathrm{V/K}^2$)		-0.10		-0.5 to -0.3

where E_g is the direct energy gap (13.2 meV for bulk Bi) at the L points of the Brillouin zone. The value of E_g is expected to increase somewhat in the nanowires due to the shift of the L-point band edges with size quantization, but that effect is on the order of a few meV in wires with 200 nm diameter, and will be neglected for this first approximation. For the holes, at the T point of the Brillouin zone, $\gamma(E_F^h)=E_F^h$.

The magnetic field, which is oriented along the wire axis [0, 0.949, 0.315], lifts the degeneracy of the three electron pockets at the L points of the Brillouin[18] zone. There are the following carrier pockets in the Fermi surface: (1) one hole pocket (h), with a cyclotron mass of $m_c^h=0.138m_0$; (2) one light-electron (Le) pocket with a cyclotron mass of $m_c^{\mathrm{Le}}=0.00211m_0$; (3) two degenerate heavy-electron (He) pockets with a cyclotron mass of $m_c^{\mathrm{He}}=0.00372m_0$, where m_0 is the free-electron mass. From Eqs. (4) and (5) and the experimental values of the SdH periods, we can thus calculate the electron and hole Fermi energies. The attribution of the SdH periods to the different pockets is made in Table I for the samples studied. Two periods, attributed to the heavy electrons and the holes, are resolved for sample 1, as is very visible in Fig. 2. Only one period is resolved for sample 2, because the quantum oscillations were weaker and more difficult to extract from the background, but that period is in good agreement with the heavy-electron period in sample 1. In the Te-doped sample, the observed SdH periods are attributed to the light and heavy electrons. The electron and hole densities can be estimated from the Fermi energies, and are also reported. Sample 1 is slightly n type, presumably due to some uncontrolled impurities. The electron density in the doped sample 3 is $5\times10^{18}\,\mathrm{cm}^{-3}$, an order of magnitude higher than the Te concentration in the melt. This is presumably due to the fact that the vapor pressure of Te is 2 orders of magnitude larger[19] than that of Bi at the same temperature.

Figure 3 shows the temperature dependence of the thermoelectric power (TEP), α, of the three samples, along with that of pure Bi. For sample 2, the data were first taken during a slow cool down of the sample at discrete temperatures stabilized with a temperature controller. This process was repeated during a warm-up cycle up to 150 K. The repeatability of the data can be inferred from the difference between the two sets of points, and is on the order of 2 μV/K. The influence of a thermal contact resistance is expected to be an overestimation of the thermal gradient as measured by the thermocouple over what is truly applied to the nanowires; this therefore results in an underestimation of the Seebeck

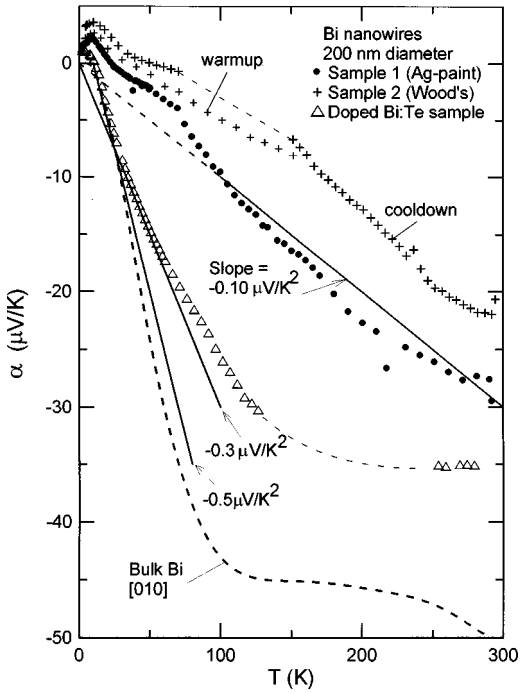

FIG. 3. The temperature dependence of the thermoelectric power of the two pure Bi nanowire arrays and the one Te-doped Bi nanowire array compared to that of bulk Bi along the bisectrix axis (dashed line). The tangent through the low-temperature data on the Te-doped sample has a slope of -0.5 $\mu\mathrm{V/K}^2$, while the data on the pure Bi sample follow a line with a -0.10 $\mu\mathrm{V/K}^2$ slope.

coefficient. The porous alumina host is amorphous, and its thermal conductivity is much lower than that of the Bi wires. The thermal conductance of the Bi nanowires dominates that of the array. One expects that the thermal contact resistance of the sample mounted with Wood's metal, which solders very well to Bi and was extensively used to contact bulk samples,[4,7] is much lower than that of the sample mounted with Ag-polymer composites. One observes that sample 2 gives the lowest absolute value of thermopower at high temperature, contrary to what is expected if thermal contact resistances were dominant. As the curves obtained with very different contact technologies give results that differ by only 8 μV/K, we estimate that this is the order of the experimental uncertainty, due to contact resistances and to sample-to-sample variations, for instance in chemical purity and carrier densities. In the pure Bi samples, the low-temperature TEP is positive and peaks at 10 K. Phonon-drag effects are known to dominate the TEP in that range, and are extremely sensitive[4] to size effects, even in samples with diameters of several mm. Above 25 K, the TEP is dominated by carrier diffusion effects, and is roughly proportional to T with an experimental slope of $\alpha/T=-0.10\,\mu\mathrm{V/K}^2$ for the pure Bi samples. The thermopower of the Te-doped sample starts at a small positive value of about 1 μV/K at 5 K, which may be due to the small thermopower in the gold voltage wires used. Between 10 and 40 K, the thermopower of the Te-doped sample has a slope of -0.50 $\mu\mathrm{V/K}^2$, much more negative than that of the pure Bi sample, in spite of the high-electron density. The absolute value of the slope of the thermopower of the doped Bi sample decreases as the temperature is increased: the curve has a tangent through the origin with a slope at -0.3 $\mu\mathrm{V/K}^2$ between 40 and 70 K. The few points taken between 250 and 300 K during sample cool down indicate that the thermopower is saturated near room temperature, as is the case for bulk Bi. We gathered data with a coarse temperature step during cool down, and with a fine step (2 to 5 K) during warm up, until the sample lost electrical contact near 130 K. Below that temperature, the data points obtained during cool down and during warm up fall on top of each other.

The thermopower of the pure Bi nanowires is the sum of the contributions of the partial thermopowers of all three carrier types, weighted by their partial electrical conductivities. Above 50 K, thermal smearing makes heavy and light electrons undistinguishable. From Eq. (3) in this paper and Eqs. (3) and (4) of Ref. 12, assuming that the mobility tensor components scale as the inverse mass tensor components, the diffusion TEP is

$$\frac{\alpha}{T}=(0.75\pm0.008)\,\frac{\alpha_e}{T}+(0.25\pm0.008)\,\frac{\alpha_h}{T}, \tag{7}$$

where the uncertainty in the coefficients reflects the different values of the ratio κ_2/κ_3, and α_e and α_h are the partial thermopowers for electrons and holes, expressed by Eq. (21) in Ref. 12 as (note that $\alpha_i=\alpha_i^0 g_{0,i}$ in Ref. 12):

$$\frac{\alpha_e}{T}=-\frac{\pi^2}{3}\,\frac{k_B}{q}\,\frac{k_B T\gamma'(E_F^e)}{\gamma(E_F^e)}, \tag{8}$$

$$\frac{\alpha_h}{T}=+\frac{\pi^2}{3}\,\frac{k_B}{q}\,\frac{k_B T}{E_F^h}. \tag{9}$$

The factor 3 in the denominator of Eqs. (8) and (9) is valid for bulk Bi, where acoustic phonon scattering dominates, but also for the nanowires, in which scattering on the wall dominates. In both cases the mean-free path is independent of temperature or Fermi energy. Calculated values for these partial thermopowers, using the value of E_F^h and E_F^e from the SdH period, are given in Table I, along with the values for pure Bi from Ref. 12. Using Eq. (7), the slope of the total thermopower of these wires can also be estimated, and is given in Table I, along with the calculated TEP of pure Bi [using Eqs. (5), (6), and (7)] along the same direction. The agreement is probably fortuitous, but indicates that the thermal contact resistance is not a major obstacle to these measurements. From Table I it is evident that the partial electron and hole thermopowers are quite large in the pure Bi samples, while the total thermopower is the difference between the two, Eq. (7), and is thus extremely sensitive to small deviations of carrier densities from those in bulk Bi. This explains the fact that the thermopower measured in these pure Bi wires is only about half that of bulk Bi. The thermopower of the Te-doped Bi sample is equal to that of the electron pockets only (neglecting again the difference between the light and heavy electrons, which, in this case, can be justified down to low temperatures because the Fermi energy is much larger than the energy splitting between the He and Le pockets), so that $\alpha/T=\alpha_e/T$ as given by Eq. (8). The calculated value of this slope is again given in Table I, and again the agreement is rather astonishingly good, given the large number of assumptions used. In real applications, material with some optimal n-type (Te is a monovalent donor[20]) and p-type (Sn is a monovalent acceptor[20]) doping level would be used, since it is shown here that the compensation effect Eq. (7) is then avoided.

Figure 4 shows the longitudinal magneto-Seebeck coefficient of pure Bi sample 2, as a function of magnetic field at temperatures ranging from 10 to 150 K. The data were taken during the same warm-up cycle as the data shown in Fig. 3. At very high values of the magnetic field, this coefficient is expected to saturate.[9] Like the zero-field thermopower, the saturation values are a combination of the electron and hole mobilities and partial thermopowers α_e and α_h. Unfortunately, the magnetic fields available to us were insufficient to saturate the longitudinal magneto-Seebeck coefficient at higher temperatures, and the fit[9] of the intermediate-field longitudinal magneto-Seebeck coefficient is not very satisfactory even in bulk Bi where the mobility values are well known. The low-temperature data in Fig. 4 do show saturation, but in that temperature range phonon-drag effects dominate. For those reasons, no further analysis of the data was attempted.

Figure 5 shows the longitudinal magneto-Seebeck coefficient of the doped Bi sample. Following the Eqs. (2) and (3) of Ref. 9, the thermopower is not expected to vary with the longitudinal field when one type of charge carriers dominates unless the Fermi energy changes. Experimentally, the relative magneto-Seebeck effect observed on the doped sample is much smaller than in the pure Bi nanowires. The small

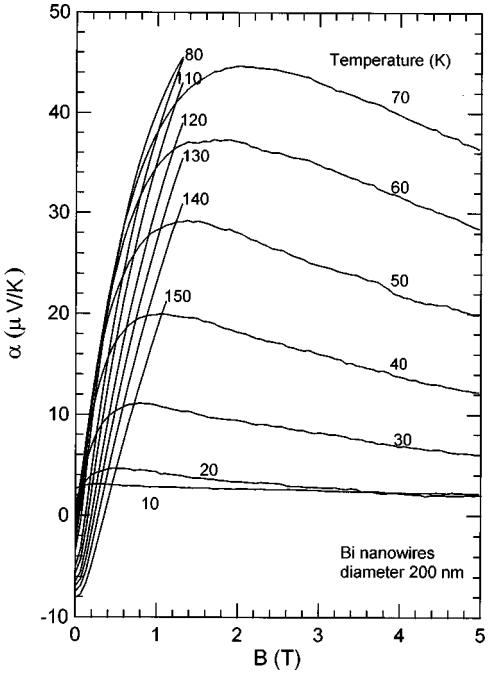

FIG. 4. Magnetic-field dependence of the longitudinal magneto-Seebeck coefficient of pure Bi sample 2, for various values of temperature.

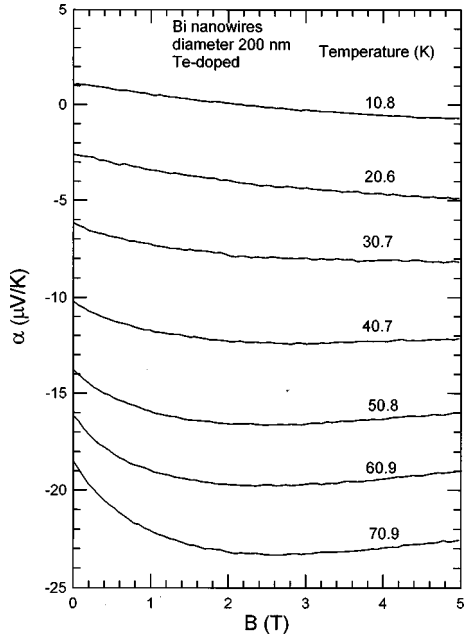

FIG. 5. Magnetic-field dependence of the longitudinal magneto-Seebeck coefficient of the Te-doped sample 3, for various values of temperature.

positive thermopower value (about $+1$ μV/K) visible at 10 K is probably again due to the gold voltage probes.

SUMMARY

In summary, we present the first thermoelectric power data taken on an array of bismuth nanowires. The results are consistent with the carrier densities deduced from the periods of the high-field Shubnikov-de Haas oscillations observed in the magnetoresistance of the nanowires. The small thermopower observed in the pure Bi samples is due to the compensation between the negative contribution of electrons and the positive contribution of holes. Much larger values of thermopower are expected in optimally doped *n*-type and *p*-type samples.

ACKNOWLEDGMENTS

The authors would like to acknowledge Professor M. S. Dresselhaus, Dr. G. Dresselhaus, and Dr. D. T. Morelli for discussions and critical reading of the manuscript.

[1] G. Dresselhaus, M. S. Dresselhaus, Z Zhang, and X. Sun, in *International Conference on Thermoelectrics, Nagoya, Japan, 1998* (IEEE, Piscataway, NJ, 1988), p. 43.
[2] C. F. Gallo, B. S. Chandrasekhar, and P. H. Sutter, J. Appl. Phys. **34**, 144 (1963).
[3] J-P. Michenaud and J-P. Issi, J. Phys. C **5**, 3061 (1972); R. Hartman, Phys. Rev. **181**, 1070 (1969); C. Uher and W. P. Pratt, Phys. Rev. Lett. **39**, 3257 (1977).
[4] J. Boxus and J-P. Issi, J. Phys. C **10**, L397 (1978).
[5] C. Uher and W. P. Pratt, J. Phys. F **8**, 1979 (1978).
[6] J-P. Issi and J. Heremans, *Proceedings of the 15th International Conference on Thermal Conductivity* (Plenum, New York, 1977); W. P. Pratt, and C. Uher, Phys. Lett. **68A**, 74 (1978).
[7] J. Boxus, C. Uher, J. Heremans, and J-P. Issi, Phys. Rev. B **23**, 449 (1981).
[8] J-P. Issi, Aust. J. Phys. **32**, 585 (1979).
[9] C. Uher and H. J. Goldsmid, Phys. Status Solidi B **64**, K25 (1974).
[10] J. H. Mangez, J-P. Issi, and J. Heremans, Phys. Rev. B **14**, 4381 (1976).
[11] O. P. Hansen, E. Cheruvier, J-P. Michenaud, and J-P. Issi, J. Phys. C **11**, 1825 (1978).
[12] J. Heremans and O. P. Hansen, J. Phys. C **12**, 3483 (1979).
[13] M. Gurvitch, J. Low Temp. Phys. **38**, 777 (1980); N. B. Brandt, D. B. Gitsu, V. A. Dolma, and Ya. G. Ponomarev, Zh. Eksp. Teor. Fiz. **92**, 913 (1987) [Sov. Phys. JETP **65**, 515 (1987)].
[14] Z. Zhang, X. Sun, M. S. Dresselhaus, J. Y. Ying, and J. Heremans, Appl. Phys. Lett. **73**, 1589 (1998).
[15] J. Heremans, C. M. Thrush, Z. Zhang, X. Sun, M. S. Dresselhaus, J. Y. Ying, and D. T. Morelli, Phys. Rev. B **58**, 10 091 (1998).
[16] J. Heremans, C. M. Thrush, B. K. Fuller, Z. Zhang, X. Sun, M. S. Dresselhaus, and J. Y. Ying, Bull. Am. Phys. Soc. **44**, 226 (1999).
[17] V. Eckstein, A. W. Lawson, and D. H. Renecker, J. Appl. Phys. **31**, 1534 (1960).
[18] V. S. Edelman, Adv. Phys. **25**, 555 (1976).
[19] S. M. Sze, *Physics of Semiconductor Devices* (Wiley-Interscience, New York, 1969).
[20] J. M. Noothoven van Goor, Philips Res. Rep. Suppl. 4 (1971).